Potential Dependent Adhesion Forces on Bare and Underpotential Deposition Modified Electrode Surfaces

Joseph M. Serafin,† Show-Jon Hsieh, Jennifer Monahan, and Andrew A. Gewirth*

Department of Chemistry and Frederick Seitz Materials Research Laboratory, University of Illinois at Urbana−Champaign, 600 South Mathews Avenue, Urbana, Illinois 61801

Received: July 7, 1998; In Final Form: September 28, 1998

Adhesion force measurements are used to determine the potential dependence of the force of adhesion between a Si_3N_4 cantilever and a Au(111) surface modified by the underpotential deposition (upd) of Bi or Cu in acid solution or by oxide formation. The measured work of adhesion is near zero for most of the potential region examined in Bi upd but rises after the formation of a full Bi monolayer. The work of adhesion is high at positive potentials for Cu upd but then decreases as the Cu partial and full monolayers are formed. The work of adhesion is low in the oxide region on Au(111) but rises following the sulfate disordering transition at 1.1 V vs NHE. These results are interpreted in terms of the degree of solvent order on the electrode surface.

1. Introduction

The composition and structure of an electrode surface determines its catalytic and electrochemical properties. Consequently, one of the main objectives of electrochemistry is the elucidation of the structure as well as the potential dependence of that structure. Adsorption on electrodes is of particular importance, as the state of the adsorbates on electrode surfaces profoundly affects their electronic and chemical properties.

One of the most precise methods for changing the composition of an electrode surface is through the underpotential deposition (upd) process.[1−3] In this procedure, monolayers or submonolayers of a foreign metal adatom are deposited on a surface at potentials positive from the reversible or Nernst potential. Because upd is driven by electronegativity (or, equivalently, work function) differences between an adatom and the surface, the process is essentially self-limiting and stops after the formation of at most two monolayers. The monolayers formed are interesting not only for their physical properties but also because of their role in electrocatalysis and the bulk deposition of metals.

The importance of anion coadsorption to the surface structural and catalytic properties of the upd adlattice has been amply demonstrated for a number of upd systems.[3] One of the problems in obtaining direct information about this coadsorption is the lack of a tool exhibiting both high spatial resolution and chemical sensitivity. The need for such a tool extends not only to the upd process but also generally to the process of adsorption on electrode surfaces, especially because the solvent is present in concentrations typically several orders of magnitude higher than any other adsorbate.

In this paper we use adhesion measurements between an atomic force microscope (AFM) tip and the electrode surface to elucidate the chemical composition in the region near the electrode surface. We show that the adhesion between a Si_3N_4 tip and a modified Au electrode surface is potential dependent.

The use of the AFM for adhesion measurements has received considerable attention recently,[4,5] and is sometimes referred to as chemical force microscopy (CFM). One of the main advantages of using an AFM, as compared to the surface force apparatus (SFA)[6] or interfacial force microscope (IFM),[7] is that the AFM probe can afford a high degree of spatial resolution. Indeed, use of specific chemical interactions have been employed for imaging in frictional force microscopy.[8−10]

In the AFM based adhesion measurements performed to date, a wealth of useful chemical information has been obtained. In a typical experiment, both the probe and sample surface are covered with a functionalized self-assembled monolayer (SAM), and the surface−surface interaction is determined. In this manner, quantities such as the surface and interfacial free energy can be obtained. The adhesion measurements can serve as sensitive probes of the variations in the chemical interactions and surface energies and have been extended to pH titrations and oxidation state dependencies.[5]

A related experimental methodology is the examination of the tip−surface approach force curves to determine the surface charge in the framework of Derjaguin−Landau−Verwey−Overbeek (DLVO) theory.[11,12] In this manner, many important values, such as the isoelectric point or point of zero charge, can be determined.[5] In the electrochemical environment, Arai and Fujihira[13] used the approaching tip−sample force profiles to determine that specific adsorption of anions had occurred.

The focus of this paper is on the use of adhesion force measurements as a probe of electrochemical events, in particular, the specific chemical interaction between a probe and the bare or adsorbate modified electrode surface. Two similar experimental approaches have been adopted by Hudson et al.[14] and Marti et al.,[10] where adhesion or friction is used to monitor potential dependent changes on the electrode. Hudson et al.[14] coated the probe and sample surface with a conducting polymer and found the adhesion to depend on the oxidation state of the polymer. This can be quite useful for imaging, as the hydrophilic and hydrophobic regions have different adhesion values with either oxidation state of the polymer, allowing for the possibility of chemical contrast frictional imaging without changing tips, thereby eliminating a complication that can make comparisons problematic. The experiments of Marti[10] investigated the frictional properties of an electrode surface under

* To whom correspondence should be addressed.
† Present address: Department of Chemistry, Clarion University of Pennsylvania, Clarion, PA 16214.

10.1021/jp982881q CCC: $15.00
Published on Web 11/10/1998

potential control, and evidence of chemical specificity was observed. In an experiment by Green et al.,[15] the oxidation state of a surface bound redox species was monitored by examining the potential dependent change in the adhesion.

One of the most significant advantages, and limitations, of adhesion based measurements is that they can be highly surface specific. We recently used the specific interaction between a Si_3N_4 cantilever and a Au surface in basic solution to probe the potential dependent adhesion between these two materials.[16] The results were interpreted on the basis of hydrogen bonding between the tip and the sample occurring when the surface was covered with OH groups. We now extend the measurements performed under basic conditions to the acid electrochemical environment. We examine the potential dependent behavior of the work of adhesion on three distinct yet related systems: upd of Bi on Au(111) in $HClO_4$, upd of Cu on Au(111) in H_2SO_4, and oxide formation on Au(111) in H_2SO_4. As discussed below, all of these systems involve the interplay of adsorbate with anion and solvent. The adhesion measurements presented here provide additional insight into the composition of the near-surface region in the electrochemical environment.

2. Experimental Section

The Au sample substrate was prepared by annealing Au coated glass (Metallhandel Schröer GMBH, Berlin) in a H_2 flame just prior to use.[17] The surface crystallinity was confirmed using the imaging mode of the AFM; this allowed for the precise positioning of the probe surface to the center of a large atomically flat crystallite. The exposed geometric area of the electrode was 0.635 cm^2. All solutions were prepared with ultrapure water (Millipore Q) and bismuth(III) oxide (99.9% Pure, Aldrich), copper(II) sulfate pentahydrate (99.999% pure, Aldrich), copper(II) chloride (99.999%, Aldrich), perchloric acid (Ultrex, Ultrapure Reagent, J. T. Baker), and sulfuric acid (Ultrex, Ultrapure Reagent, J. T. Baker). All reagents were used without subsequent purification. Potential control was maintained with a CV-27 potentiostat (Bioanalytical Systems) using a standard three-electrode configuration. The counter electrode was a flame annealed Au wire, and the reference electrode was fabricated from an oxidized Au wire. For Cu upd measurements, the counter and reference electrodes were formed from a Cu wire. Absolute voltage calibration was achieved by comparison of voltammetry in the sample cell with voltammetry obtained using a $Hg/HgSO_4$ reference electrode. All solutions were deoxygenated prior to use, and the adhesion force measurements were performed under a slight positive pressure of N_2. All potentials reported are relative to NHE.

The adhesive measurements were performed in a commercial AFM apparatus (Molecular Imaging) using commercial control and data acquisition electronics (Nanoscope III, Digital Instruments). With this apparatus, the electrode is fixed in space and the probe surface is scanned. The working electrode was clamped in space with a Teflon cell that contained the supporting electrolyte solution.

The probe surface was a commercial Si_3N_4 AFM tip (Digital Instruments, oxide sharpened). The surface of the Si_3N_4 is positively charged under the experimental conditions (pH = 1−2). The deflection sensitivity of the instrument was calibrated against the linear response in the region of constant compliance for every run, and the scanning piezoelectric crystal was calibrated by imaging a grating of known dimensions. V-shaped cantilevers were used for these experiments, as the spring constants of the torsional modes are large for this geometry. The variation in the spring constant between AFM wafers is notoriously high, and it is thus necessary to calibrate the spring constant of the cantilevers. Fortunately, the variation in the spring constant across a wafer is quite small and can be quite satisfactorily obtained from averaging a few sample cantilevers on a given wafer. The force constants of the cantilevers were estimated from the resonance frequency of the cantilever and the manufacturer's specifications of the dimensions of the cantilever legs.[18] All of the cantilevers used in this study were gold coated to increase the reflectivity of the probe diode beam. Without the reflective gold coating, the optical interference from the gold electrode resulted in a large oscillatory background signal at the position sensitive detector, which hindered discrimination of the cantilever deflection. The effect of the gold reflective coating was accounted for in the calculation of the force constant.[19]

The adhesion force, F_{ad}, between a probe and sample surface can be related to the work of adhesion, W_{ad}, using Johnson−Kendall−Roberts (JKR) theory.[20] Here, F_{ad} and W_{ad} are related as

$$F_{ad} = -{}^3/_2 \pi R_T W_{ad} \quad (1)$$

where R_T is the radius of curvature of the probe surface. Thus, in this work, the physically important parameter is not actually the magnitude of the force of adhesion but rather the force of the adhesion normalized by the radius of curvature of the tip surface. It is this quantity which can be directly related to W_{ad}. The method used to determine the radius of curvature will be discussed below, but it should be noted that with this method the actual spring constant does not enter in the actual force to radius value, F/R.

Determination of the Radius of Curvature of the Probe Surface. It is desirable to have an in situ method for the determination of the radius of curvature of the probe surface. One recently developed approach uses long-range double layer forces to determine this radius.[21] However, this method may not be appropriate for small distances. We adopted a methodology similar to that proposed by Hutter and Bechhoefer,[22] where the shorter range van der Waals force is used for the calibration. A nonretarded Hamaker constant, A_H, of 13×10^{-20} J[23] is estimated from an average geometric mean of the Si_3N_4/water/Si_3N_4 A_H value of $(5-6) \times 10^{-20}$ J and an A_H of $(25-40) \times 10^{-20}$ J for gold/water/gold.[24] The van der Waals interaction energy between a sphere and a surface is described in the nonretarded limit as

$$W_{vdw}(d) = +A_H R_T/6d \quad (2)$$

where d is the sphere−surface distance.[25] Equation 2 is valid for the case where $d \ll R_T$. The force on the sphere is

$$F_{vdw}(d) = -A_H R_T/6d^2 \quad (3)$$

For the passive cantilevers used in AFM force measurements, there exists a region of mechanical instability when the force gradient of the potential exceeds the spring constant of the cantilever, k_s,

$$\partial F/\partial d = k_s \quad (4)$$

At this instability, the probe surface will jump into contact with the surface with a characteristic "snap in" distance, d_s, which is obtained from combining eqs 3 and 4,

$$d_s = (A_H R_T/3k_s)^{1/3} \quad (5)$$

Thus, R_T, is determined over a short-range measurement, namely, d_s. Equation 5 can be rearranged such that

$$R_T = 3k_s d_s^{\,3}/A_H \quad (6)$$

Finally, the adhesion force is determined by

$$F_{ad} = Dk_s \quad (7)$$

where D is the displacement of the probe surface. Then, combining eqs 1, 6, and 7 yields

$$F_{ad}/R_T = -{}^3/_2\pi W_{ad} = DA_H/3d_s^{\,3} \quad (8)$$

with no dependence on k_s.

3. Results

A. Bismuth Underpotential Deposition on Au(111) in $HClO_4$. Shown in Figure 1 is a cyclic voltammogram of Bi upd obtained in 0.1 M $HClO_4$ in the AFM instrument. This voltammetry is somewhat less resolved than that obtained in cells where conditions of strict deoxygenation can be obtained, but compares favorably with published voltammetry,[26] especially in the stripping region. In Figure 1, potential region A corresponds to bare Au(111), where the perchlorate anion is known not to associate with the surface. Sweeping the potential negatively to potential region B, the surface now has an adsorbed layer of OH^- present,[26] as well as partial coverage of Bi in a (2 $\times$ 2) lattice.[27,28] After the second underpotential deposition peak is region C, where the surface is covered with a ($p \times \sqrt{3}$) monolayer of Bi, and no OH^- is present. The same behavior is observed when the potential is swept positive, where potential region D corresponds to the removal of the complete monolayer of Bi to a partial coverage of both Bi and OH^-.

The adhesion force is obtained from the force vs cantilever displacement profiles. Figure 2 shows a typical force measurement taken at 0.25 V, which corresponds to region C. The dashed line is the tip surface approach, and the zero of the force curve corresponds to the interaction at infinite separation, which for practical purposes will usually extend a few tens of nanometers. The solid line is the tip surface retraction, and the pull-off force is determined when the Si_3N_4 surface is pulled off the surface of the electrode once the restoring force of the cantilever exceeds the adhesion interaction. The adhesion measurement is derived from the difference between the zero and minimum of the retraction curve.

Between the different potential regions a marked variation in the adhesion force was observed. Shown in Figure 3 are three sample adhesion graphs from potential regions A−C. While there is essentially no adhesion observed in regions A and B, the adhesion in region C is significantly larger than in the other potential regions. Figure 4 shows the potential dependence of this change in adhesion for cathodic (Figure 4A) and anodic (Figure 4B) potential sweeps for five different measurements with different tips and surfaces during the Bi upd process. Figure 4 shows that the change in adhesion force closely corresponds to the electrochemical features. The adhesion is essentially zero until reaching a potential between 0.3 and 0.35 V vs NHE, where the work of adhesion rises to a value between 0.03 and 0.12 N/m depending on the specific measurement. This potential corresponds to the potential at which the ($p \times \sqrt{3}$) full monolayer of Bi is formed on the Au(111) electrode surface. When the potential scan is reversed,

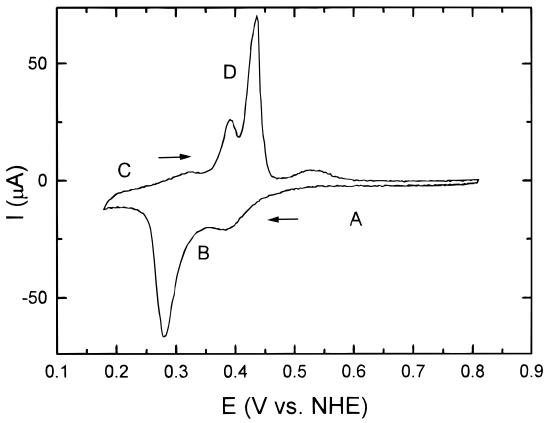

Figure 1. Cyclic voltammogram of Bi upd on Au(111) in 0.1 M $HClO_4$. Bi concentration was 2 mM. Scan rate was 25 mV/s. The letters denote different potential regions described in the text.

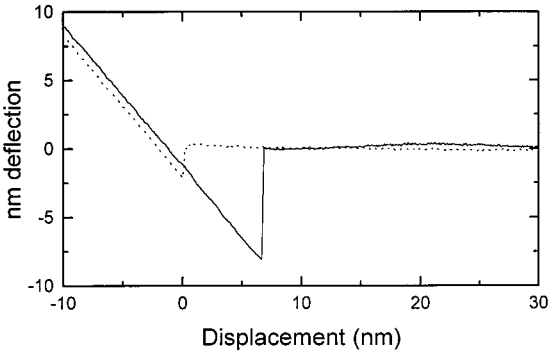

Figure 2. Representative tip−surface approach and retraction force curve obtained at 0.25 V vs NHE in a solution containing 0.1 M $HClO_4$ and 2 mM Bi^{3+}. The dashed line denotes the tip−surface approach curve showing the characteristic jump to contact at 0 nm displacement. The solid line shows the tip−surface retraction curve. Reported adhesion forces are determined from the difference between the retraction curve minimum and the force at large separation.

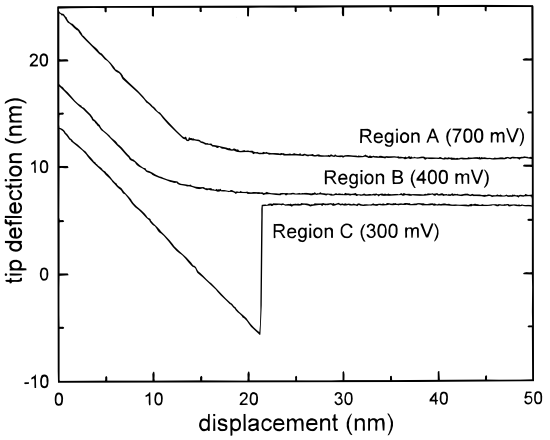

Figure 3. Tip deflection vs pull out displacement curves for potential regions A, B, and C on Au(111) in a solution containing 0.1 M $HClO_4$ and 2 mM Bi^{3+}. The zero of displacement corresponds to the onset of constant compliance for the tip−surface approach curves. The curves have been offset for clarity.

the full monolayer is removed from the surface at 0.4 V vs NHE. Figure 4B shows that this potential corresponds to that where reduction in the adhesive force between the tip and surface is also observed. The adhesion then remains essentially at zero upon further anodic potential excursion.

Figure 4 also shows that while all tip−sample combinations follow the general trends described above, there is considerable

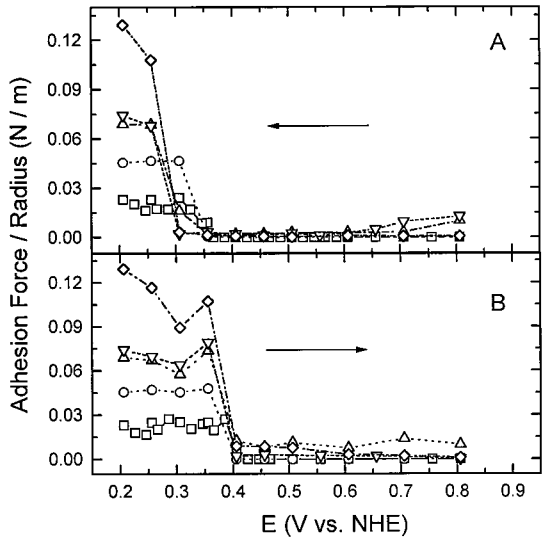

Figure 4. Adhesion Force divided by tip radius vs potential plots for Bi upd on Au(111) in cathodic (A) and anodic (B) potential sweeps. Solution conditions are as in Figure 3. The five different symbols denote results for five different tip/surface combinations.

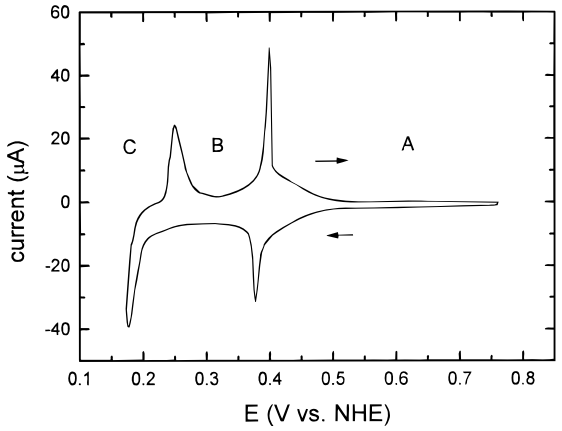

Figure 5. Cyclic voltammogram for Cu upd in a solution containing 2 mM $CuSO_4$ and 0.1 M H_2SO_4 on Au(111) obtained in the AFM cell. Scan rate was 10 mVs^{-1}.

variation in the actual measured W_{ad} between different tips and surfaces. Typically, position and clarity of upd voltammetric features provide a good measure of the degree of order and cleanliness in the upd system. We could not correlate changes in the measured work of adhesion with changes in the appearance of the Bi upd voltammetry. The variation in W_{ad} found in this system should be contrasted with that observed in basic solution following oxide formation voltammetry on Au(111),[16] where different values for the maximum of the work of adhesion were within 10% of each other; the over 400% relative error found here with Bi is considerably greater.

B. Copper Underpotential Deposition on Au(111) in H_2SO_4. To examine the origin of the variation of W_{ad} with the potential seen in Figure 4, we examined another upd system: Cu upd on Au(111) in H_2SO_4. The Cu upd system in sulfate on Au(111) is perhaps the most studied[29−31] and best understood of the upd systems and forms an archetype for examining anion−adatom coadsorption behavior.[32,33] Shown in Figure 5 is a cyclic voltammogram of Cu upd[17] obtained in the AFM instrument. Looking at Figure 5, potential region A corresponds to a surface consisting of gold with a disordered array of sulfate ion on the surface, the amount of which is potential dependent.[32] STM images obtained at very positive potentials (ca. 1.1 V vs

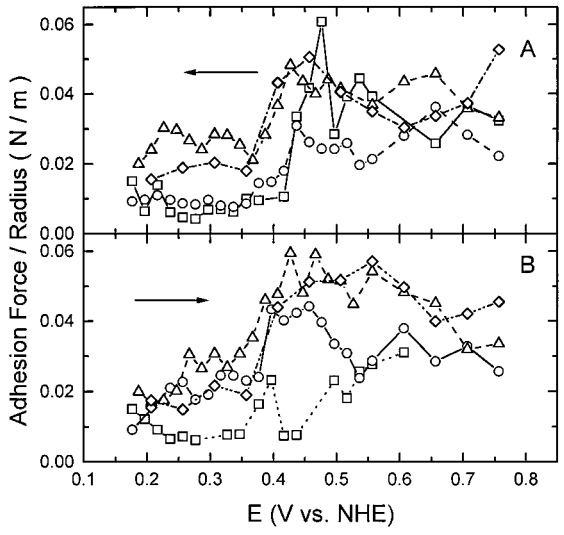

Figure 6. Adhesion Force divided by tip radius plots vs potential for Cu upd on Au(111) in cathodic (A) and anodic (B) potential sweeps. Solution conditions are as in Figure 5. The four different symbols denote results for four different tip/surface combinations.

NHE)[34,35] show a $(\sqrt{3} \times \sqrt{7})$ overlayer structure which has been interpreted as arising from water and sulfate coadsorbed on the Au(111) surface.[36] However, this structure is not present between 1.1 and 0.4 V vs NHE, and only bare Au(111) is observed because the disordered sulfate is not imaged. Scanning the potential negatively through the first upd peak to potential region B gives rise to a new structure now known to correspond to a two-thirds coverage of Cu arranged in a honeycomb pattern and a one-third coverage of bisulfate arranged in a $(\sqrt{3} \times \sqrt{3})$-$R30°$ pattern.[31] A more negative potential scan into region C gives rise to a pseudomorphic (1×1) overlayer.[29] If the potential is moved 50 mV to even more negative values, bulk deposition of Cu occurs. Reversing the sweep direction and moving to more positive potentials leads to recovery of the two-thirds coverage and bare Au regions.

Between the different potential regions a marked variation in the adhesion force was also observed in this system. Figure 6 shows the potential dependence of the adhesion force for four different surface−tip combinations for both cathodic (Figure 6A) and anodic (Figure 6B) potential sweeps. Note that the adhesion force closely corresponds to some of the electrochemical features. However, the behavior here is different from that observed with Bi above. In particular, W_{ad} appears to drop as we move from region A into region B. There is no increase in W_{ad} moving into region C, which corresponds to full monolayer formation. Finally, the overall value of W_{ad} is small, and there is considerably more scatter in the data relative in the bare Au region (region A) relative to that found for Bi.

We also attempted to study Cu upd in 0.01 M $HClO_4$ with a small amount of Cl^- (4 mM) present. The presence of Cl^- is known to lead to a (5×5) adlattice[37] related to Cl^- participation in the structure. Measurement of W_{ad} vs the potential in this system did in fact roughly follow these features in the voltammetry in that the adhesion was high at positive potentials and then dropped by approximately a factor of 2 upon sweeping through the first (most positive) upd peak in a cathodic scan. However, the presence of Cl^- ions caused two difficulties in interpreting the data. The first was that addition of Cl^- gave rise to a very large snap in distance, which implies an unphysically large (ca. 1000 nm) tip radius. The second effect was that the force curves exhibited structure at short distances. Similar results have been reported by Senden and Drummond

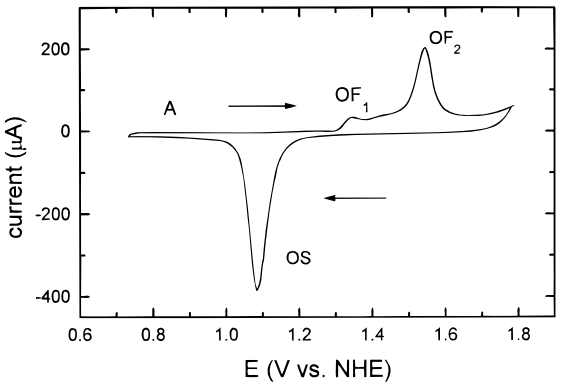

Figure 7. Cyclic voltammogram showing the Au oxide region on Au(111) in a solution containing 0.01 M H_2SO_4. Scan rate was 50 mVs^{-1}.

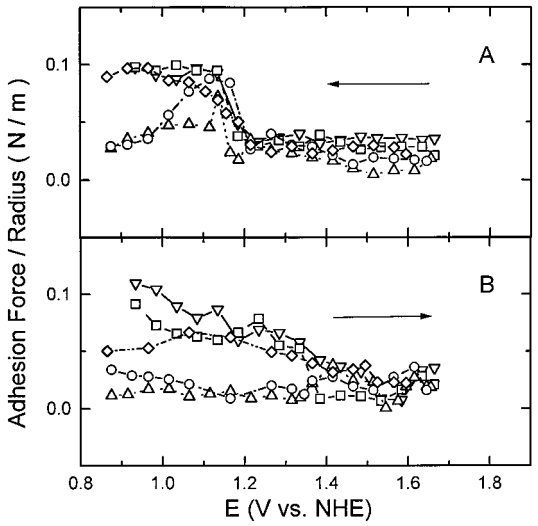

Figure 8. Adhesion force divided by tip radius plots for Au oxide formation on Au(111) in cathodic (A) and anodic (B) potential sweeps. Solution conditions are as in Figure 7. The five different symbols denote results for five different tip/sample combinations.

for Si_3N_4 tips and mica surfaces in the presence of NaCl.[38] It seems as if the Cl^- ion is being involved in some complicated manner mediating the adhesive interaction, possibly through adsorption of this ion onto the tip. Thus measurements of W_{ad} in this system are not possible without a change in tip chemistry.

C. H_2SO_4 on Au(111). Finally, we examined the behavior of a bare Au surface in the absence of upd. Shown in Figure 7 is a cyclic voltammogram for H_2SO_4 on Au(111) obtained in the AFM sample cell. Above 1.1 V in potential region A there exists the $(\sqrt{3} \times \sqrt{7})$ sulfate anion−water structure on the gold surface discussed above. As the potential is swept positive, the oxidative features OF_1 and OF_2 which begin around 1.35 V correspond to the formation of gold hydroxide and oxide, respectively.[39] After the potential sweep is reversed the oxide stripping peak, OS, occurs at ∼1.1 V, and the surface is once again left bare.

Figure 8 shows the potential dependence of W_{ad} for a series of measurements using different tips and substrates. Figure 8A shows that the adhesion force is relatively low as the potential is scanned from 1.6 V to ca. 1.1 V. At this point, W_{ad} rises and remains high. Reversing the potential sweep leads to a drop in W_{ad} between 1.2 and 1.4 V. As with the Bi W_{ad} vs E plots the low-adhesion data are relatively constant between different tip−sample measurements, but appreciable scatter occurs in the more adhesive region of the plot.

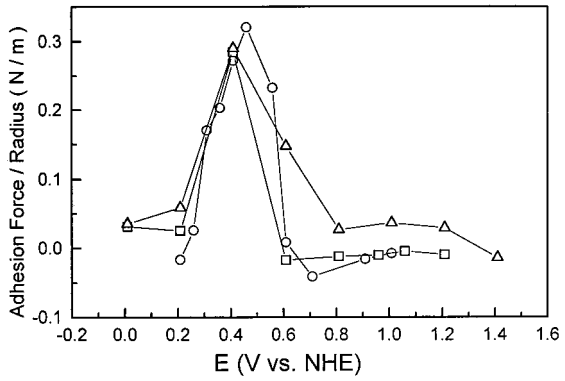

Figure 9. Results of three different measurements of adhesion force divided by tip radius as a function of applied potential for oxide formation on Au(111) in 0.01 M NaOH.

4. Discussion

The results presented above show that W_{ad} is a potential dependent quantity in acid solution and can map changes in the structure of the surface and interface. The results presented above are noteworthy for their magnitude, potential dependence, and lack of reproducibility in magnitude in regions of high adhesion. Ideally, these data should correlate with changes in the electrode surface structure or near-surface structure as controlled by the applied potential and solution composition. It should be stressed that all of the experimental runs had similar qualitative trends and differed only in magnitude.

We have previously examined the interaction of the Si_3N_4 tip with Au(111) in NaOH.[16] Shown in Figure 9 are W_{ad} vs E plots from three different trials (i.e., different tips, different crystallites, etc.). Figure 9 shows that while W_{ad} is low at both high and low potentials, it rises to a maximum of about 0.3 N/m in the intermediate region. It is noteworthy to compare the magnitudes of the adhesion force for the different trials and realize that they are quite close (ca. 10%). In a basic aqueous environment, the probe surface presents primarily $Si-O^-$ functionality, and we interpreted the results to indicate that the variation in the adhesion was primarily due to the interaction of the probe surface with specifically adsorbed OH groups on the surface, with the specific interaction ascribed to hydrogen bonding on the basis of its magnitude. The results presented in this paper above are noteworthy from this perspective in that W_{ad} is considerably smaller and also exhibits considerably more variance relative to the study in the basic environment.

The work of adhesion, W_{ad}, between two surfaces can be quantified as

$$W_{ad} = \gamma_{ss'} + \gamma_{ts'} - \gamma_{ts} \tag{9}$$

where $\gamma_{ss'}$ is the interfacial free energy of the electrode surface and the solvent, $\gamma_{ts'}$ is the interfacial free energy of the probe tip surface and the solvent, and γ_{ts} in the interfacial free energy of the electrode and probe surfaces. Equivalently, W_{ad} can also be expressed as

$$W_{ad} = W_{vdw} + W_{se} + W_{hb} \tag{10}$$

where W_{vdw} is the work of adhesion due to van der Waals and other electrostatic interactions, W_{se} is the work done in solvent exclusion, and W_{hb} is the work done in hydrogen bonding or other direct specific interactions between tip and surface.

W_{hb} is the interaction which is commonly implicated in contrast between modified tips and surfaces of appropriate functionality.[40] However, our tips are not functionalized, and

we are performing measurements in the acid electrochemical environment where they are fully protonated.[38] There is no reason to expect that any of the modified surfaces we produce through the upd process or by oxide formation will have a greater specific interaction with the tip than any other. W_{hb} is thus not likely the interaction responsible for the potential-dependent changes in W_{ad}.

van der Waals and other electrostatic interactions make up another class of possible contributors to W_{ad}. Changes in the repulsive double layer force between tip and surface have been used to determine the percent ionization of as surface as a function of pH.[41] However, those measurements were carried out in a relatively dilute electrolyte. Experimentally, we can determine whether van der Waals and electrostatic interactions are important through recourse to the approach curves where a positive deflection on approach prior to jump-to-contact is typically interpreted in terms of electrostatic interactions.[42] For both the Cu upd and the H_2SO_4 cases there is virtually no positive deflection upon approach throughout the entire potential range examined. This suggests that for the sulfate electrolyte, the charge on the surface is effectively screened. We speculate that the origin of this screening behavior is the relatively strong adsorption of sulfate to the Au(111) electrode surface, but a detailed explanation of this behavior remains to be obtained. Hence for these two measurements in sulfate electrolyte, W_{ad} is not affected by van der Waals and electrostatic interactions and W_{vdw} is not the origin of the changes in W_{ad} measured here.

For the Bi case, however, W_{vdw} is not negligible at positive potentials in dilute electrolyte. While measurements obtained at 0.2 V in concentrated (0.1 M) electrolyte as shown in Figure 2 evince essentially no van der Waals or electrostatic interaction (no positive deflection on approach), such is not the case at more positive potentials in solutions diluted by an order of magnitude. Here, we observed considerable deflection (where however, W_{ad} is small). Some of this deflection is discernible even in the higher concentration pull-off curves shown in Figure 3. However, in the negative potential region between 0.2 and 0.3 V, where W_{ad} takes nonzero values, W_{vdw} measured in either concentration of electrolyte was essentially the same and essentially zero. Equally significant, the magnitude and potential-dependent behavior of W_{ad} was the same in either concentration. That W_{vdw} is not negligible in the positive potential region in this system may have to do with the lack of specific adsorption of perchlorate to Au(111), which would then leave the surface charge unscreened. However, the lack of any positive deflection in the approach curve at negative potentials makes W_{vdw} an unlikely source of the potential-dependent changes in W_{ad}.

To understand the potential-dependent changes in W_{ad}, we must make recourse to a detailed description of the surface chemistry of each of these systems. In the case of Bi in $HClO_4$ at potentials positive of the potential of zero charge (pzc) which is around 0.55 V vs NHE,[43,44] $HClO_4$ is thought to form a clathrate structure[45] leading to an ice-like water structure as seen in infrared measurements.[46] In pure $HClO_4$ this ice-like structure is destroyed as the potential is moved to more negative values. However, 0.55 V is at the start of the Bi upd prewave which we have associated with the onset of hydroxide adsorption [26] and is generally associated with an ordering transition on the surface.[47] Moving to more negative values, the (2×2)-Bi adlayer forms. We have shown that this adlayer is coadsorbed with OH^-. It is reasonable to expect that the OH^- orders the solvent and/or anion above the surface and tightly holds the water in place. However, moving to more negative values still leads to the $(p \times \sqrt{3})$-Bi phase and desorption of the hydroxide. At this point we anticipate that neither water nor anion is strongly held. We note the appearance of the $(p \times \sqrt{3})$-Bi phase is coincident with the development of higher W_{ad} values.

In the sulfate systems at very positive potentials the surface is covered with a layer of oxide or hydroxide. As the potential is swept more negative, the surface forms a $(\sqrt{3} \times \sqrt{7})$ sulfate phase above 1.1 V. IR measurements indicate that this phase features a strongly held anion−water complex featuring ordered anion and solvent.[36] Moving the potential more negative from 1.1 V, the anion disorders on the surface and water becomes less tightly held. 1.1 V is also the onset of the region of high adhesion.

Upd of Cu causes the readsorption of sulfate and most likely a consequent reordering of solvent above the surface. Sulfate is adsorbed atop the Cu upd adlayer,[31] even in the 1×1 pseudomorphic phase. Sulfate is also adsorbed atop bulk Cu.[48,49] Cu is also interesting because of indications that it forms a layer of water or hydroxide even in acidic solutions.[50] The implication then is that water is ordered above it too.

From the above descriptions of surface chemistry, a cogent picture of the origin of the increased W_{ad} emerges. When the surface either strongly adsorbs water or anion and water the adhesion is low. When the anion is either expelled from the surface or the surface is disordered, then the adhesion is high. Essentially then the W_{ad} we measure is probing the reorganization energy of water and/or anion as the tip moves away from the surface. In systems where the water is tightly held to the Au surface, this reorganization energy is small. On the other hand, when water is not tightly held, the reorganization energy is high and appears as the W_{ad} measured here. To this end, the relevant energy is that which describes the transition between hydrophobic and hydrophilic behavior. Based on SFA apparatus and contact angle measurements, this energy - - the 'water adhesion tension' - - is believed to be on the order of 0.03 N/m.[51] This number is of the correct magnitude to account for the change in W_{ad} seen here.

We noted before that while the low adhesion measurements were relatively constant and reproducible, such was not the case for regions of high adhesion. If the high adhesion regions involve solvent reorganization, the exact energy required for this will be exquisitely dependent on solvent purity, homogeneity of the surface in the region of the tip, and other factors such as minor potential-dependent changes in the characteristics of the tip due to impurities where, for example, changes in potential may change the effective pH near the surface and hence the tip. The degree of care required to obtain reproducible measurements in the high adhesion region would then be extreme.

Recent experiments have unambiguously elucidated the role of solvation forces or solvent exclusion by comparing systems where the surface chemistries remain the same, but the solvent is changed.[52] Such an approach is not well suited to electrochemical systems, where varying the solvent while maintaining the same surface chemistry is difficult. It should also be noted, that the same limitations in varying the solvent also applies to studies of biomolecular interaction under physiological conditions. Elucidating the solvent interactions terms in simple electrochemical systems will be invaluable in evaluating those same terms when considering biomolecular interactions.[53]

5. Conclusion

The results presented in this paper show that the potential-dependent variation in the work of adhesion between an AFM tip and a surface in the electrochemical environment can be a

sensitive probe of the state of the electrode surface. The results presented here have been interpreted as suggesting that W_{ad} is mainly due to the work of solvent ordering. The work due to solvent ordering is greatest when water is not ordered into an ice-like or rigid structure on the Au surface. This rigidity may be accompanied by or induced by anion ordering on the surface.

Acknowledgment. This work was funded by Department of Energy Grant DE-FG02-91ER45349 through the Materials Research Laboratory at the University of Illinois.

References and Notes

(1) Kolb, D. M. In *Advances in Electrochemistry and Electrochemical Engineering*; Gerischer, H., Tobias, C. W., Eds.; Wiley: New York, 1978; Vol. 11.
(2) Adzic, R. R. In *Advances in Electrochemistry and Electrochemical Engineering*; Gerischer, H., Tobias, C. W., Eds.; Wiley-Interscience: New York, 1984; Vol. 13.
(3) Aramata, A. In *Modern Aspects of Electrochemistry*; Bockris, J., Ed.; Plenum Press: New York, 1997; Vol. 31.
(4) Carpick, R. W.; Salmeron, M. *Chem. Rev.* **1997**, *97*, 1163−1194.
(5) Noy, A.; Vezenov, D. V.; Lieber, C. M. *Annu. Rev. Mater. Sci.* **1997**, *27*, 381−421.
(6) Israelachvili, J. *Intermolecular and Surface Forces*; 2nd ed.; Academic Press: San Diego, 1994.
(7) Thomas, R. C.; Houston, J. E.; Crooks, R. M.; Kim, T.; Michalske, T. A. *J. Am. Chem. Soc.* **1995**, *117*, 38.
(8) Green, J.-B. D.; McDermott, M. T.; Porter, M. D.; Siperko, L. M. *J. Phys. Chem.* **1995**, *99*, 10960.
(9) Marti, A.; Hahner, G.; Spencer, N. D. *Langmuir* **1995**, *11*, 4632.
(10) Weilandt, E.; Menck, A.; Binggeli, M.; Marti, O. In *Nanoscale Probes of the Solid/Liquid Interface*; Gewirth, A. A., Siegenthaler, H., Eds.; Kluer Academic Publishers: Boston, 1995; Vol. 288.
(11) Derjaguin, B. V.; Landau, L. *ACTA Physiochim. URSS* **1941**, *14*, 633.
(12) Verway, E. J. W.; Overbeek, J. T. G. *Theroy of Stability of Lyophobic Colloids*; Elsevier: Amsterdam, 1948.
(13) Arai, T.; Fujihira, M. *J. Vac. Sci. Technol. B* **1996**, *14*, 1378.
(14) Hudson, J. E.; Abruna, H. D. *J. Am. Chem. Soc.* **1996**, *118*, 6303.
(15) Green, J.-B. D.; McDermott, M. T.; Porter, M. D. *J. Phys. Chem.* **1996**, *100*, 13342.
(16) Serafin, J. M.; Gewirth, A. A. *J. Phys. Chem. B* **1997**, *101*, 10833−10838.
(17) Will, T.; Dietterle, M.; Kolb, D. M. In *Nanoscale Probes of the Solid−Liquid Interface*; Gewirth, A. A., Siegenthaler, H., Eds.; Kluwer: Dordrecht, 1995; Vol. 228.
(18) Cleveland, J. P.; Manne, S.; Bocek, D.; Hansma, P. K. *Rev. Sci. Inst.* **1993**, *64*, 403.
(19) Sader, J. E.; Larson, I.; Mulvaney, P.; White, L. R. *Rev. Sci. Inst.* **1995**, *66*, 3789.
(20) Johnson, K. C.; Kendall, K.; Roberts, A. D. *Proc. R. Soc. London, Ser. A.* **1971**, *324*, 301.
(21) Drummond, C. J.; Senden, T. J. *Colloids Surfaces A: Physiochem. Eng. Aspects* **1994**, *87*, 217.
(22) Hutter, J. L.; Bechhoefer, J. *Rev. Sci. Inst.* **1993**, *64*, 1868.
(23) Ackler, H. D.; French, R. H.; Chiang, Y. M. *J. Colloid Interface Sci.* **1996**, *179*, 460.
(24) Schrader, M. E. *J. Colloid Interface Sci.* **1984**, *100*, 372.
(25) Derjaguin, B. V. *Kolloid Zeits* **1934**, *69*, 155.
(26) Niece, B. K.; Gewirth, A. A. *Langmuir* **1996**, *12*, 4909−4913.
(27) Chen, C.-H.; Kepler, K. D.; Gewirth, A. A.; Ocko, B. M.; Wang, J. *J. Phys. Chem.* **1993**, *97*, 7290.
(28) Chen, C.-h. C.; Gewirth, A. A. *J. Am. Chem. Soc.* **1992**, *114*, 5439−40.
(29) Magnussen, O. M.; Hotlos, J.; Nichols, R. J.; Kolb, D. M. *Phys. Rev. Lett.* **1990**, *63*, 2929.
(30) Manne, S.; Hansma, P. K.; Massie, J.; Elings, V. B.; Gewirth, A. A. *Science* **1991**, *251*, 183.
(31) Toney, M. F.; Howard, J. N.; Richer, J.; Borges, G. L.; Gordon, J. G.; Melroy, O. R. *Phys. Rev. Lett.* **1995**, *75*, 4472−4475.
(32) Shi, Z. C.; Wu, S. J.; Lipkowski, J. *Electrochim. Acta* **1995**, *40*, 9−15.
(33) Legault, M.; Blum, L.; Huckaby, D. A. *J. Electroanal. Chem.* **1996**, *409*, 79−86.
(34) Magnussen, O. M.; Hagebock, J.; Hotlos, J.; Behm, R. J. *Faraday Discuss.* **1992**, *94*, 399−400.
(35) Edens, G. J.; Gao, X. P.; Weaver, M. J. *J. Electroanal. Chem.* **1994**, *375*, 357−366.
(36) Ataka, K.; Osawa, M. *Langmuir* **1998**, *14*, 951−959.
(37) Batina, N.; Will, T.; Kolb, D. M. *Faraday Discuss.* **1992**, *94*, 93−106.
(38) Senden, T. J.; Drummond, C. J. *Colloids Surfaces A: Physiochem. Eng. Aspects* **1995**, *94*, 29.
(39) Hamelin, A. *J. Electroanal. Chem.* **1996**, *407*, 1.
(40) Noy, A.; Sanders, C. H.; Vezenov, D. V.; Wong, S. S.; Lieber, C. M. *Langmuir* **1998**, *14*, 1508−11.
(41) Hu, K.; Bard, A. J. *Langmuir* **1997**, *13*, 5114−5119.
(42) Butt, H.-J. *Biophys. J.* **1991**, *60*, 1438.
(43) Angerstein-Kozlowska, H.; Conway, B. E.; Hamelin, A.; Stoicoviciu, L. *Electrochim. Acta* **1986**, *31*, 1051.
(44) Angerstein-Kozlowska, H.; Conway, B. E.; Hamelin, A.; Stoicoviciu, L. *J. Electronal. Chem.* **1987**, *228*, 429.
(45) Borkowska, Z.; Stimming, U. In *Structure of Electrified Interfaces*; Lipkowski, J., Ross, P. N., Eds.; VCH: New York, 1993.
(46) Ataka, K.; Yotsuyanagi, T.; Osawa, M. *J. Phys. Chem.* **1996**, *100*, 10664−10672.
(47) Huckaby, D. A.; Blum, L. *J. Electroanal. Chem.* **1991**, *315*, 255.
(48) Ehlers, C. B.; Villegas, I.; Stickney, J. L. *J. Electroanal. Chem.* **1990**, *284*, 403.
(49) Ehlers, C. B.; Stickney, J. L. *Surf. Sci.* **1990**, *239*, 85.
(50) Lagraff, J. R.; Gewirth, A. A. *Surf. Sci.* **1995**, *326*, L 461-L 466.
(51) Vogler, E. A. *Advances in Colloid & Interface Science* **1998**, *74*, 69−117.
(52) Sinniah, S. K.; Steel, A. B.; Miller, C. J.; Reutt-Robey, J. E. *J. Am. Chem. Soc.* **1996**, *118*, 8925.
(53) Israelachvili, J.; Wennerstrom, H. *Nature* **1996**, *379*, 219−225.